

Elsevier Editorial System(tm) for Microvascular Research
Manuscript Draft

Manuscript Number: MVR-10-132R1

Title: Hemodynamic analysis of capillary in finger nail-fold using computational fluid dynamics and image estimation

Article Type: Regular Article

Keywords: Red blood cell, Blood flow, Hemodynamic analysis, Velocity measurement

Corresponding Author: Dr. Tzungchi Huang, Ph.D.

Corresponding Author's Institution: Department of Biomedical Imaging and Radiological Science, China Medical University

First Author: Tzu-Ching Shih

Order of Authors: Tzu-Ching Shih; Geoffrey Zhang; Chih-Chieh Wu; Hung-Da Hsiao; Tung-Hsin Wu; Kang-Ping Lin; Tzungchi Huang, Ph.D.

Abstract: Red blood cell (RBC) dynamics in capillaries is a useful diagnostic tool for many diseases. Previous study showed that optical flow estimation (OFE) is capable of accurately calculating RBC velocities using image registration technique. The computational fluid dynamics (CFD) method is explored in this study to calculate the RBC velocity in capillaries of finger nail-fold for six cases. The two-dimensional capillary images were reconstructed to three-dimensional, assuming circular cross sections. The no-slip boundary conditions were applied on the vessel walls. The initial velocity of the RBC going into each capillary was calculated by OFE. The velocities of multiple points along each capillary calculated by CFD, VCFD, were compared with OFE calculations, VOFE. The calculated RBC velocity was in the range of 56-685 $\mu\text{m/s}$. The average difference (VCFD-VOFE) with one standard deviation is $-2.66 \pm 18.61 \mu\text{m/s}$ for all the 48 calculation points, and $0.03 \pm 0.12 \mu\text{m/s}$ for all except one points (47 points), indicating that CFD can provide a reasonable accuracy in RBC velocity calculation in finger nail-fold capillaries.

Suggested Reviewers:

Hemodynamic analysis of capillary in finger nail-fold using computational fluid dynamics and image estimation

Tzu-Ching Shih¹, Geoffrey Zhang², Chih-Chieh Wu³, Hung-Da Hsiao⁴, Tung-Hsin Wu⁵,

Kang-Ping Lin⁶, Tzung-Chi Huang^{1,*}

¹Department of Biomedical Imaging and Radiological Science, China Medical University, Taiwan

²Radiation Oncology, H. Lee Moffitt Cancer Center and Research Institute, Tampa, Florida, USA

³Instrument Technology Research Center, National Applied Research Laboratories, Taiwan

⁴National Center for High-Performance Computing, Taiwan

⁵Department of Biomedical Imaging and Radiological Sciences, National Yang Ming University, Taiwan

⁶Department of Electrical Engineering, Chung Yuan Christian University, Taiwan

*Corresponding author, Tzung-Chi Huang, address: 91, Hsueh-Shih Road, Taichung, 404 Taiwan, phone: (886)4-2205-2121 #7623, fax: (886)4-2233-4175, Email: tzungchi.huang@mail.cmu.edu.tw

Abstract

Red blood cell (RBC) dynamics in capillaries is a useful diagnostic tool for many diseases. Previous study showed that optical flow estimation (OFE) is capable of accurately calculating RBC velocities using image registration technique. The computational fluid dynamics (CFD) method is explored in this study to calculate the RBC velocity in capillaries of finger nail-fold for six cases. The **two**-dimensional capillary images were reconstructed to **three**-dimensional, assuming circular cross sections. The no-slip boundary conditions were applied on the vessel walls. The initial velocity of the RBC going into each capillary was calculated by OFE. The velocities of multiple points along each capillary calculated by CFD, V_{CFD} , were compared with OFE calculations, V_{OFE} . The calculated RBC velocity was in the range of 56-685 $\mu\text{m/s}$. The average difference ($V_{CFD}-V_{OFE}$) with one standard deviation is $-2.66 \pm 18.61 \mu\text{m/s}$ for all the 48 calculation points, and $0.03 \pm 0.12 \mu\text{m/s}$ for all except one points (47 points),

indicating that CFD can provide a reasonable accuracy in RBC velocity calculation in finger nail-fold capillaries.

Introduction

Microcirculation plays an essential role in biological tissues to supply oxygen and nutritive substances and to remove waste products. Red blood cell (RBC) dynamics in capillaries has been well understood in relation to certain diseases, such as Raynaud's phenomenon^{1,2}, hypertension^{3,4} or diabetes^{5,6}, for examples. To provide the blood flow information, we previously developed an RBC velocity measurement system based on the optical flow estimation (OFE) method⁷⁻⁹ which processes capillaroscopy images of finger nail-fold.

The computational fluid dynamics (CFD) approach to calculate RBC velocity consists of the searching of flow patterns in a given geometry and applying the initial/boundary conditions for flow variables. The CFD techniques were used to investigate the hemodynamic factors, such as deformation of erythrocytes (*i.e.*, red blood cells, RBCs)¹⁰⁻¹², blood viscosity^{11,13}, wall shear stress¹³⁻¹⁵, and blood velocity^{11,13,17,18} in the complex three-dimensional(3D) blood microvessels. Those studies demonstrated that the CFD approach can provide not only the motion information of blood flow but also the deformation of RBCs flowing in the microvessels. Furthermore, Sun and Munn¹⁶ used the lattice Boltzmann simulation to analyze the efficient flow of RBCs and white blood cells (WBCs) passing through the microvessels. They also provided the complete solution of the blood flow field and quantification of the RBC and WBC forces in complex vessel networks. Thus, the numerical modeling can provide a useful tool to analyze the blood flow in a complex vessel geometry.

In this study, CFD was applied to estimate the capillary blood flow in finger nail-fold based on the optical images acquired by the video capillaroscopy system⁷. The CFD performance, and the comparison between CFD and OFE calculations are presented. The validation of the method is analyzed in this paper.

Materials and Methods

Capillaroscopy system

The lighting and sampling scheme of the capillaroscopy system, which consists of an optical microscope, a charge coupled device (CCD) video camera, an LCD monitor, and a video recorder. The closed-circuit video system M320 (JMC Corporation, Kyoto, Japan) is shown in Fig. 1. The video recorder acquires real-time blood flow video of microcirculation at $\times 380$ magnification, with a spatial resolution of $1.42 \mu\text{m}$ and image

sampling rate of 30 frames per second. The static image pixel matrix size is 720×480. Each video sequence was recorded for a total of 10 seconds. Image signals are also output to a computer via an image capture card. White LED light sources are embedded around the objective lens. The light sources illustrate with a specific oblique angle in order to minimize the specular reflection.

Image Data

Six right-handed healthy male human (age of 20–30 years old) participated in the study. Subjects were recruited from colleagues, and were diagnosed with no Raynaud’s phenomenon, hypertension or diabetes within 6-months. In each stage of flow condition, three sections of the capillary for RBC velocity were examined including arteriolar limb (section I), curve (section II) and venular limb (section III). Several points were selected in each section. The segmentation of the three sections is shown in Fig. 2. A RBE image acquired by the capillaroscopy system is shown in Fig. 3 as an example. Average RBC velocities for all the 3 sections and at selected points were calculated through image processing for the duration of 10 seconds.

CFD Blood Flow Estimation - Finger Nail-fold Capillary Geometric Reconstruction

To perform a CFD simulation of blood flow in a finger nail-fold capillary, a three-dimensional description of the vessel lumen is required. Finger nail-fold capillary images, acquired from the capillary blood flow video recorder, were processed to extract geometric shapes representing the vessel lumen boundary of the capillaries. The capillary wall was reconstructed based on the two-dimensional (2D) geometry of the finger nail-fold capillary, assuming circular cross sections. **The length of each section and the width of the cross section along the nail-fold capillary in 2D images were used for the characteristic values of the 3D capillary geometric dimensions.** The reconstruction geometry of a nail-fold capillary wall inherently determines the blood flow movement. As demonstrated in Fig. 4, **a 3D finger nail fold capillary wall for Case 1 was** reconstructed by the commercial software ESI-GEOM (ESI Group, Huntsville, AL, USA) for the CFD simulation. The nail-fold capillary walls were assumed to be rigid in simulations. The flow-in velocity at the beginning of the arteriolar section, V_{in} , calculated by the optical flow estimation method (as shown in Table 1-2), was assigned as the inlet velocity in the reconstructed 3D vessel, and the velocity calculation by CFD for the other seven selected points was based on this inlet velocity.

CFD Blood Flow Estimation - Governing Equations for Blood Flow in Nail-fold Capillaries

The blood flow in the finger nail-fold capillary was modeled by employing the incompressible Navier-Stokes equations as follows:

$$\rho \left(\frac{\partial u}{\partial t} + u \frac{\partial u}{\partial x} + v \frac{\partial u}{\partial y} + w \frac{\partial u}{\partial z} \right) + \frac{\partial p}{\partial x} = \mu \left(\frac{\partial^2 u}{\partial x^2} + \frac{\partial^2 u}{\partial y^2} + \frac{\partial^2 u}{\partial z^2} \right) + \rho g_x \quad (1)$$

$$\rho \left(\frac{\partial v}{\partial t} + u \frac{\partial v}{\partial x} + v \frac{\partial v}{\partial y} + w \frac{\partial v}{\partial z} \right) + \frac{\partial p}{\partial y} = \mu \left(\frac{\partial^2 v}{\partial x^2} + \frac{\partial^2 v}{\partial y^2} + \frac{\partial^2 v}{\partial z^2} \right) + \rho g_y \quad (2)$$

$$\rho \left(\frac{\partial w}{\partial t} + u \frac{\partial w}{\partial x} + v \frac{\partial w}{\partial y} + w \frac{\partial w}{\partial z} \right) + \frac{\partial p}{\partial z} = \mu \left(\frac{\partial^2 w}{\partial x^2} + \frac{\partial^2 w}{\partial y^2} + \frac{\partial^2 w}{\partial z^2} \right) + \rho g_z \quad (3)$$

, where t is time, ρ is the density, p is the pressure, μ is the **blood** viscosity. The blood velocity components in x , y and z directions are denoted as u , v and w . The components of gravitational acceleration in these directions are denoted by g_x , g_y , and g_z , respectively. The above differential equations were implemented in each node of a 3D mesh. The gravity effect was ignored in this study. The no-slip boundary conditions were applied on the vessel walls and a uniform velocity profile was used at the inlet. The blood was approximated as a Newtonian fluid with a density of **1050** kg/m³ and a dynamic viscosity of 0.035 kg/m/s (Cole and Watterson 2003)¹⁷.

Visual inspection validation

In this study, the blood flow calculated using OFE estimation was regarded as the standard, and the validation of CFD simulation is based on the comparison to the OFE calculation. The accuracy of the OFE estimation was assessed by visual inspection (VI) method¹⁸. The frame-to-frame VI method calculates the blood flow by observing the movement of cells or plasma gaps between two continuous frames. With greatly improved image contrast after image pre-processing, the frame-to-frame VI method can estimate the blood flow velocity with a high accuracy. A drawback of the VI method is that the estimation of RBC movement between two frames is subjective and varies with

observers. Such observer dependency was eased by visually measuring the velocity from the slopes of stripes on the space-time diagram and averaging it with the result of the frame-to-frame method to obtain the reference velocity. In fact, the combination of two VI methods was used to validate OFE method.

Results

In the CFD simulations, the inlet velocity was the only parameter estimated by the OFE. **Figure 6 shows that the outlet velocities by the CFD modeling with different element numbers for Case 1. The calculated velocities of various grid sizes were almost identical to each other at each distance, indicating that the CFD numerical results is grid independent. Figure 7 shows** the velocity contours in the 3D capillary calculated by CFD at selected points for **Case 1**. By adjusting the z coordinates, an optimal point can be found such that the velocity calculated by CFD is close to that measured by the OFE method. For instance, for velocity V1 in **Case 1**, the relative difference between the CFD calculation and the OFE calculation was less than 0.2% at a z value of either 0.83 or -0.83 μm . The Nail-fold capillary velocities simulated by the CFD method did not differ appreciably from those calculated by the OFE method with the same xy coordinates, except for V6 in Case 1 (Table 1). This difference may be due to that the cross section at V6 may not be circular and it is much narrower in the z direction. The cross section area was thus smaller than it appeared. The CFD method underestimated velocity using a larger cross section area based on the circular cross section assumption.

Table 2 summarizes the comparison for the 6 cases studied. The largest difference between the CFD and OFE calculated RBC velocity appeared in Case 1 due to the largest difference at V6. At 4 μm away from the center of vessel, the relative differences of velocity between the CFD calculation and the OFE calculation for all other points were less than 0.1%. The overall average difference with one standard deviation for all the data points, total of 48, is $-2.66 \pm 18.61 \mu\text{m/s}$, while the corresponding value if V6 in Case 1 is excluded is $0.03 \pm 0.12 \mu\text{m/s}$.

Discussion

Using the inlet velocity estimated by the OFE method, the CFD method gave a reasonably good agreement for blood flow velocities of most other selected points with the OFE calculations. At the same depth (z value), the difference of the velocity between the CFD method and the OFE method was small. Case 1 is a good example of such comparison (Table1).

The CFD method may underestimate the velocity for points that are close to the

capillary wall in the 3rd dimension direction (z direction) due to overestimation of the cross section. The point V6 in **Case 1** is such an example.

The capillary diameter change determines the variation of RBC velocity in the finger nail-fold capillary. When the capillary diameter variation is small, the velocity variation is small. It is also noticed when the variation of the size of the capillary diameter was smaller in the arteriolar and venular sections, the CFD method predicted the velocity in the finger fold capillary accurately.

In our six numerical simulation cases, with the capillary diameter ranging from 8.98 to 21.72 μm , the calculated maximum velocity was about 685.35 $\mu\text{m/s}$. For the six cases, the maximum Reynolds number was less than 0.003, indicating smooth laminar flow in all the CFD calculations. As the agreement between OFE and CFD calculations were good for these points, the CFD method thus has larger errors for these very high blood flow velocities. The reason may be that the blood in narrow capillary vessels (internal diameter < 500 μm) behaves as a non-Newtonian fluid. In such blood vessels, the viscosity of blood depends upon the vessel diameter. This flow behavior is known as the Fåhræus-Lindqvist effect¹⁹. As blood flow in small vessels with internal diameter of 20-500 μm displaying a multiphase suspension of deformable particles, a continuous model of blood flow is not adequate if the motion of individual red blood cells are in suspension flow. In our CFD simulations, the fluid of blood was modeled as single viscous phase. This may lead to errors in velocity estimation when the capillary vessels are narrow.

Conclusion

In this study, we presented an image-based CFD modeling with realistic finger nail-fold capillaries. The CFD simulation results demonstrate that the model is capable of predicting the velocity distributions with a reasonable accuracy.

Reference

- [1] Wollersheim H., Reyenga J. and Thien T . Laser Doppler velocimetry of fingertips during heat provocation in normals and in patients with Raynaud's phenomenon Scand. J. Clin. Lab. Invest. 48, 91–5(1988).
- [2] Bertuglia S., Leger P., Colantuoni A., Coppini G., Bendayan P. and Boccalon H.

- Different flowmotion patterns inhealthy controls and patients with Raynaud's phenomenon Technol, Health Care 7 ,113–23 (1999).
- [3] E. Bonacci, N. Santacroce, N. D'Amico, and R. Mattace., Nail-fold capillaroscopy in the study of microcirculation in elderly hypertensive patients, Arch. Gerontol. Geriatr. suppl. 5, 79-83 (1996).
- [4] Cesarone M R, Incandela L, Ledda A, De Sanctis M T,Steigerwalt R, Pellegrini L, Bucci M, Belcaro G andCiccarelli R. Pressure and microcirculatory effects of treatment with lercanidipine in hypertensive patients and invascular patients with hypertension Angiology 51, 53–63 (2000).
- [5] Chung-Hsing Chang, Rong-Kung Tsai, Wen-Chuan Wu, Song-Ling Kuo, and Hsin-Su Yu., Use of dynamic capillaroscopy for studying cutaneous microcirculation in patients with diabetes mellitus, Mircrovascular Research 53, 121-127 (1997).
- [6] E. Tibiriçá, E. Rodrigues, R.A. Cobas and M.B. Gomes., Endothelial function in patients with type 1 diabetes evaluated by skin capillary recruitment, Mircrovascular Research 73, 107-112 (2007).
- [7] Chih-Chieh Wu, Geoffrey Zhang, Tzung-Chi Huangc, Kang-Ping Lin, Red Blood Cell Velocity Measurements of Complete Capillary in Finger Nail-fold Using Optical Flow Estimation, Mircrovascular Research 78 , 63-68 (2009).
- [8] Horn, B.K.P., Schunck, B.G., 1981. Determining optical flow. Artif. Intell. Med. 17,185–203.
- [9] Tzung-Chi Huang, Wen-Chen Lin, Chih-Chieh Wu, Geoffrey Zhang, Kang-Ping Lin, Experimental estimation of blood flow velocity through simulation of intravital microscopic imaging in micro-vessels by different image processing methods, Mircrovascular Research, doi:10.1016/j.mvr.2010.07.007.

- [10] A. Jafari, P. Zamnkhan, S.M. Mousavi, and P. Kolari, Numerical investigation of blood flow Part II: capillaries, *Communications in Nonlinear Science and Numerical Simulation* 14, 1396-1402 (2009).
- [11] S.K. Doddi and P. Bagchi, Three-dimensional computational modeling of multiple deformable cells flowing in microvessels, *Physical Review E* 79, 046318(14) (2009).
- [12] T.W. Secomb, B. Styp-Rekowska, and A.R. Pries, Two-dimensional simulation of red blood cell deformation and lateral migration in microvessels, *Annals of Biomedical Engineering* 35, 755-765 (2007).
- [13] N. Filipovic, A. Tsuda, G.S. Lee, L.F. Miele, M. Lin, M.A. Konerding, and S.J. Mentzer, Computational flow dynamics in a geometric model of intussusceptive angiogenesis, *Microvascular Research* 78, 286-293 (2009).
- [14] R.W. Lyczkowski, B.R. Alevriadou, M. Horner, C.B. Panchal, and S.G. Shroff, Application of multiphase computational fluid dynamics to analyze monocyte adhesion, *Annals of Biomedical Engineering* 37, 1516-1533 (2009).
- [15] J. Jung and A. Hassanein, Three-phase CFD analytical modeling of blood flow, *Medical Engineering and Physics* 30, 91-103 (2008).
- [16] C. Sun and L.L. Munn, Lattice Boltzmann simulation of blood flow in digitized vessels networks, *Computers and Mathematics with Applications* 55, 1594-1600 (2008).
- [17] J.S. Cole and J.K. Watterson, Blood flow characteristics in a femoral artery bypass graft, *Developments in Chemical Engineering and Mineral Processing*, 11, 15-28 (2003).
- [18] Klyszcz T, Jünger M, Jung F and Zeintl H, Cap image – a new kind of computer-assisted video image analysis system for dynamic capillary microscopy (in

German) Biomed Tech (Berl), 42, 168–75 (1997).

[19] Fåharaeus R and Lindqvist T. The viscosity of the blood in narrow capillary tubes.

Am J Physiol., 96, 562-68 (1931).

Table 1. Blood flow estimation for Case 1 as an example. The largest discrepancy point is in bold fonts.

Case 1	Average velocity by CFD	Average velocity by OFE	$V_{CFD}-V_{OFE}$
	($\mu\text{m/s}$)	($\mu\text{m/s}$)	($\mu\text{m/s}$)
<u>V_{in}</u>	191.70	191.70	< 0.01
<u>V₁</u>	280.70	280.73	-0.03
<u>V₂</u>	330.57	330.58	> -0.01
<u>V₃</u>	300.32	300.33	-0.01
<u>V₄</u>	418.76	418.76	> -0.01
<u>V₅</u>	515.46	515.46	> -0.01
<u>V₆</u>	314.58	443.47	-128.89
<u>V_{out}</u>	214.28	214.28	> -0.01
<u>average</u>	320.80	336.91	-16.12
<u>stdev</u>	105.33	113.76	45.57

Table 2. Comparison summary for the 6 cases studied. The average differences (Mean diff) between the CFD and the OFE calculated velocities ($V_{CFD}-V_{OFE}$) and one standard deviation (stdev) of the differences for all the points in each case were listed in this table.

Case	1	2	3	4	5	6
Mean diff	-16.12	0.20	< 0.01	> -0.01	> -0.01	> -0.01
stdev	45.57	0.28	< 0.01	< 0.01	< 0.01	< 0.01

Figure Legends

Fig.1. Capillaroscopy system for lighting and a sampling. M320 (JMC Corporation, Kyoto, Japan) uses a closed-circuit video system consisting of a CCD video

camera, a LCD monitor, and a video recorder.

Fig.2. Definition of arteriolar limb (section I), curve segment (section II) and venular limb (section III).

Fig.3. Red blood cell flow image for **Case 1** from the capillaroscopy system.

Fig.4. 3D capillary wall reconstruction based on the 2D finger nail-fold capillary image of Case 1.

Fig.5. Accuracy of optical flow estimation. The results of visual inspection were regarded as the reference for OF. Data from 6 capillaries in resting condition were presented.

Fig.6. The outlet velocities with different element numbers for Case 1.

Fig.7. The velocity contours on the cross-sectional plane for **Case 1** at selected points.

Figure

Figure 1



Figure 2

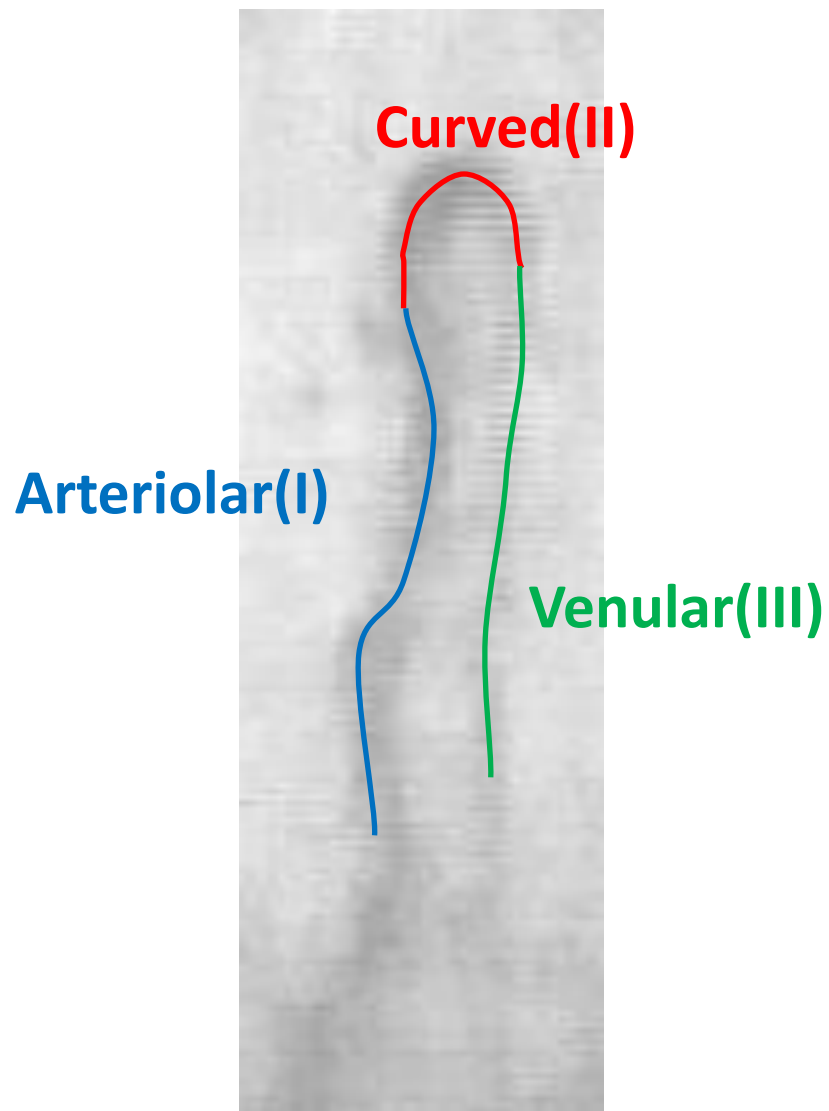


Figure 3



Figure 4

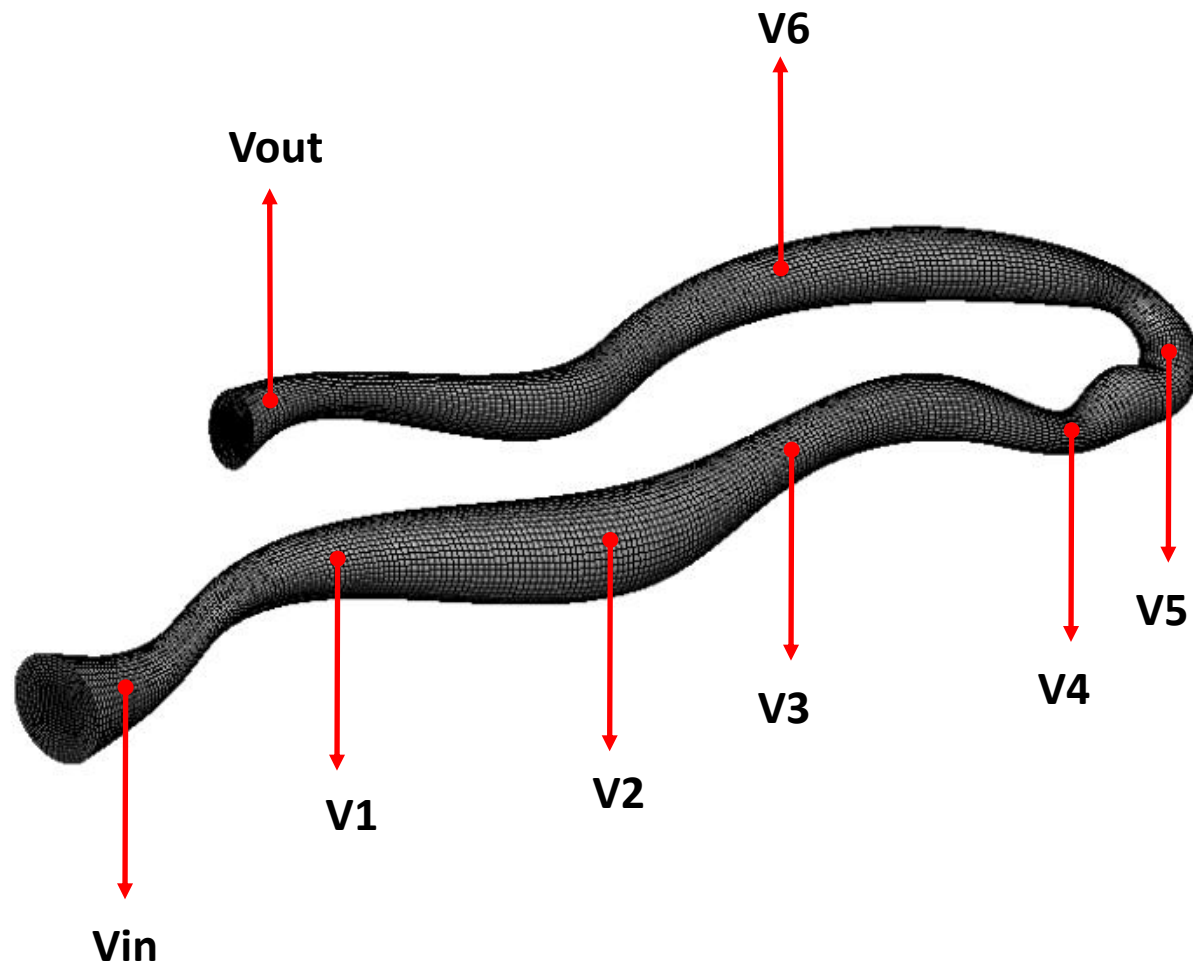


Figure 5

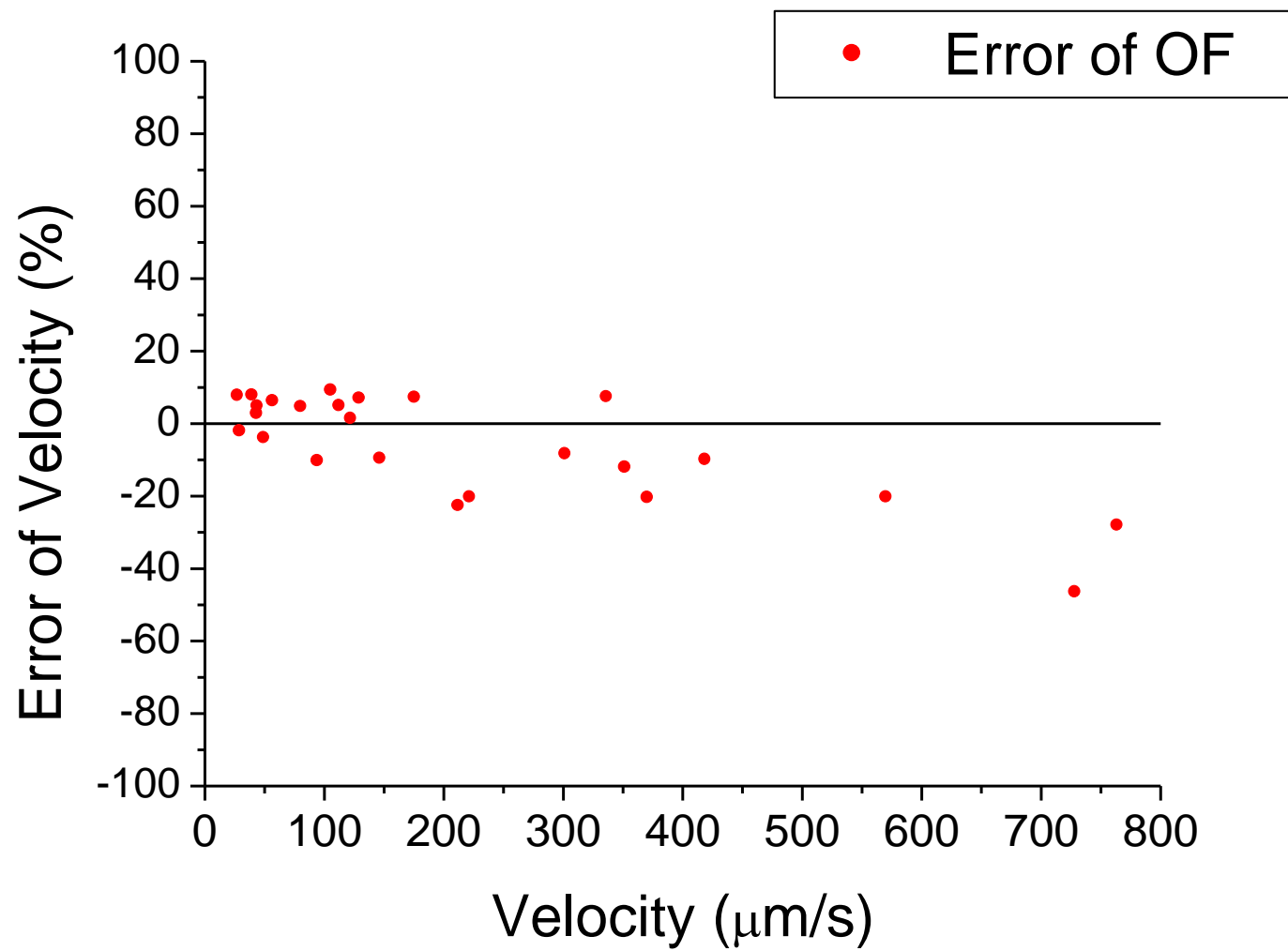


Figure 6

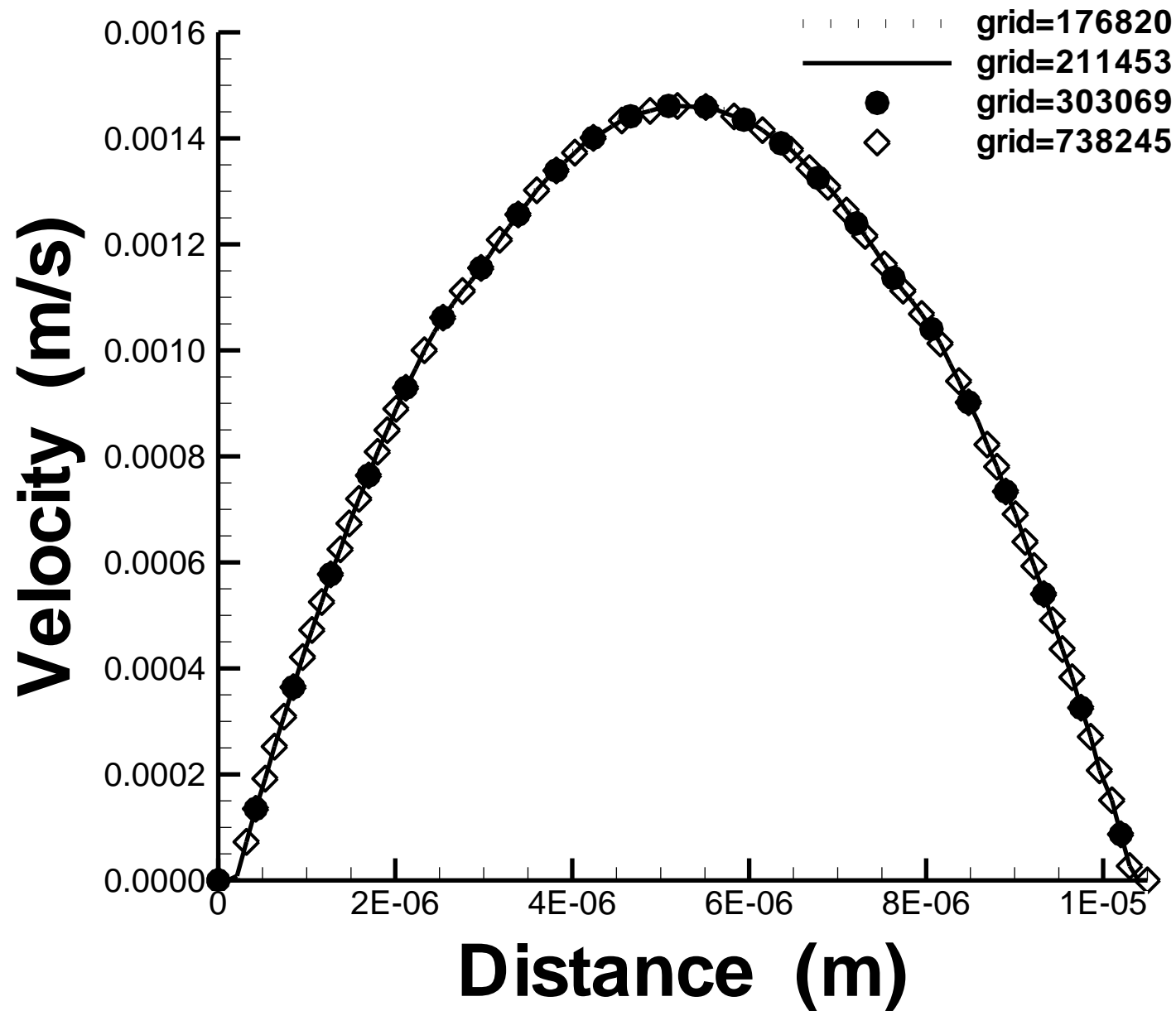


Figure 7

